

# The Impact of Fluctuations on QCD Matter\*

TINA KATHARINA HERBST<sup>a</sup>, JAN M. PAWLOWSKI<sup>b,c</sup>

AND

BERND-JOCHEN SCHAEFER<sup>a,d</sup>

<sup>a</sup> Institut für Physik, Karl-Franzens-Universität Graz, A-8010 Graz

<sup>b</sup> Institut für Theoretische Physik, Universität Heidelberg, D-62910 Heidelberg

<sup>c</sup> ExtreMe Matter Institute EMMI, GSI Helmholtzzentrum für  
Schwerionenforschung mbH, D-64291 Darmstadt

<sup>d</sup> Institut für Theoretische Physik, Justus-Liebig-Universität Gießen, D-35392  
Gießen

We study the effect of quantum and thermal fluctuations as well as the mass dependence of the phase structure of QCD at finite temperature and density within a dynamical Polyakov-loop-extended quark-meson model. The glue dynamics is simulated by the Polyakov-loop potential, also including the back-coupling of the matter sector to the glue dynamics. In the chiral limit, the chiral phase transition at large chemical potential and low temperature splits into two transition branches. For non-vanishing pion masses the chiral transition at small chemical potential changes from a phase transition to a crossover. We close with a discussion of a systematical improvement of the current model towards full QCD.

PACS numbers: 11.30.Rd, 64.60.ae, 12.38.Aw, 11.10.Wx

## 1. Introduction

Over the past two decades, much progress has been made experimentally and theoretically in our understanding of the phase structure of strongly-interacting matter [1]. This has been achieved in a combination of first principle continuum computations in QCD, see e.g. [2], lattice simulations,

---

\* Presented at the HIC for FAIR Workshop and XXVIII Max Born Symposium “Three Days on Quarkyonic Island”, Wrocław, May 19-21, 2011.

see e.g. [3, 4, 5], as well as computations in low energy effective models for QCD, see e.g. [6, 7, 8, 9, 10, 11]. At vanishing chemical potential it is established by now that there are two crossover transitions at similar temperatures, see e.g. [4, 5, 12]. Presently, it is still much under debate whether the two transitions coincide over the whole phase diagram or deviate at some chemical potential, leave aside the phase structure at larger chemical potential. In lattice simulations progress is hampered by the sign problem at finite chemical potential. The sign problem does not affect the continuum approaches which, however, have to deal with the increase of relevant degrees of freedom and fluctuations as well as the strong correlations at increasing density.

In this context it has been argued that the QCD effective models can be understood as well-controlled approximations of full first principle functional approaches to QCD, see [2, 13]. This connection allows to successively constrain and finally determine the sensitive model parameters, and hence to gain qualitatively on predictive power within these models. In turn, the models provide a more direct access and understanding of the mechanisms at work for e.g. the chiral and confinement/deconfinement dynamics, see e.g. [14, 15]. The Polyakov-extended quark-meson (PQM) model [7] is specifically well-adapted to the embedding into first principle approaches to QCD. By now it is well-studied also beyond the mean-field level at vanishing [16] and finite density [13, 17, 18, 19]. In this model the matter fluctuations are included directly within a fully non-perturbative functional renormalization group (FRG) approach, for reviews on QCD and QCD-effective models see [20, 21, 22, 23, 24, 25].

In Polyakov-extended models (part of) the glue dynamics is included with a Polyakov-loop potential in the free energy. This potential is usually constrained with the expectation value and thermodynamics of lattice Yang-Mills (YM) theory [9, 10]. Clearly, this does not completely fix the potential and the phase structure is sensitive to the chosen potential, see e.g. [26]. This necessitates a better determination of the potential. Corrections due to matter fluctuations have been computed in [7], reviewed in [27], and have been confirmed at vanishing temperature with a direct comparison of the Polyakov-loop potentials in Yang-Mills theory [28] and QCD [12]. Further work aiming at the determination also at finite chemical potential is in progress. In summary, the PQM model provides us with a good approximation of low energy QCD at not too large chemical potential, and its direct relation to continuum QCD approaches allows us to strengthen this relation successively.

In the present contribution we study the interrelation between chiral symmetry breaking, its restoration at large temperatures and/or chemical potential and the confinement/deconfinement transition within the dynam-

$$\partial_t \Gamma_k[\phi] = \frac{1}{2} \text{[Gluon loop]} - \text{[Ghost loop]} - \text{[Meson loop]} + \frac{1}{2} \text{[Quark loop]}$$

Fig. 1. RG flow for QCD, including gluon, ghost, meson and quark contributions, respectively.

ical two-flavour PQM model. We map out the full phase diagram and also provide a conservative estimate for the possible emergence of a critical endpoint. Further insights into the mechanisms at work are extracted by varying the explicit chiral symmetry breaking parameter, and hence the Goldstone-boson (pion) mass.

## 2. QCD flows and the matter back-coupling

The dynamical Polyakov-extended quark-meson model used in the present contribution consists of a Yukawa-type model of propagating quarks and mesons (pions  $\vec{\pi}$  and sigma  $\sigma$ ). As a low-energy effective model of QCD it is formed dynamically when fully taking into account the four-fermi interaction that arises from quark and gluon fluctuations. The mesonic resonances that dynamically form at lower energies, in particular in the  $s$ -channel of the four-fermi interaction, lead to effective low-energy degrees of freedom, the mesons. In the flow equation approach this is described by dynamical hadronization, see [29, 30, 22, 31]. This approach to QCD has been put forward for QCD in [12, 32] and is reviewed in [2].

The present dynamical PQM model is discussed in detail in [13], including its direct connection to the FRG approach to QCD. The flow equation for the free energy of QCD is shown in Fig. 1. It is important to emphasize that the depicted flow is exact, no higher loop diagrams are missing. Here,  $\Gamma_k[\phi]$  stands for the effective action in the presence of an infrared cut-off scale  $k$  and the free energy is given by the effective action evaluated at the equation of motion. For each degree of freedom a fully dressed one-loop structure emerges. For example, the first two loops for the gluons and ghosts comprise the pure glue sector in QCD: the full gluon and ghost propagators are screened in the presence of dynamical quarks and mesons, respectively.

An example for the matter contribution to the glue propagator is shown in Fig. 2 with the vacuum polarisation. The quark loop screens the gluon propagator, and in particular with increasing density the in-medium effects get larger. This has crucial effects, such as the reduction of the deconfinement transition temperature of the pure YM system when full QCD,

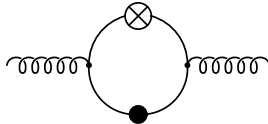


Fig. 2. Quark loop correction to the gluon propagator contributing to the matter back-coupling to the gauge sector present in full QCD.

including the dynamical quarks and meson, is considered.

The simple additive structure has important consequences for the PQM model. We can easily identify the different parts of the model in terms of full QCD fluctuations. For example, the fluctuating quark-meson sector of the model is given by the last two diagrams in Fig. 1. In other words, removing the glue sector in Fig. 1 leaves us with a dynamical quark-meson model, for a review see [24]. In turn, the glue and ghost loops in Fig. 1, evaluated in the background of a Polyakov-loop  $\Phi$ , give the Polyakov-loop potential in full QCD. This potential only agrees with the Yang-Mills potential if we neglect the matter fluctuations, such as the vacuum polarisation depicted in Fig. 2. This entails that with Fig. 2 we have access to the change of the Polyakov-loop potential in the presence of matter fluctuations.

It is precisely this simple structure which has been used in [7] for a phenomenological estimate of the matter back-coupling to the glue sector. On the practical level, the back-coupling changes the dynamical Yang-Mills scale  $\Lambda_{\text{YM}}$ , present in the gluon and ghost propagators, to the dynamical QCD scale  $\Lambda_{\text{QCD}}$ . In the Polyakov-loop potential this scale manifests itself in the critical temperature  $T_0$ . Therefore, in full QCD this parameter receives a flavour and chemical potential dependence via the vacuum polarisation, see Fig. 2, leading to  $T_0(N_f, \mu)$  [7]. By now, we also have access to the full QCD potential at vanishing chemical potential derived from solving the fully coupled QCD flows [2, 12, 33]. This result confirms the phenomenological estimate in [7], and will soon be extended to finite chemical potential, thus resolving the current ambiguity in the Polyakov-loop potential in the Polyakov-loop extended models.

The discussion above allows us to put forward the flow equation of QCD where the gluonic degrees of freedom have been integrated out. This leads to a flow for the free energy which only involves the last two loops in Fig. 1 and the first two loops lead to the Polyakov-loop glue potential  $\Omega_{\text{glue}}$ . They also lead to modifications of the matter interaction which is included in the initial conditions in the quark-meson sector that capture the correct vacuum physics. Ignoring the additional modification of the quark and meson dispersion this leads us finally to the flow equation [16, 13] for the

QCD free energy  $\Omega_{\text{QCD},k} = \Omega_k$ ,

$$k\partial_k\Omega_k(\sigma, \vec{\pi}, \Phi, \bar{\Phi}) = \frac{k^5}{12\pi^2} \left\{ \frac{1}{E_\sigma} \coth\left(\frac{E_\sigma}{2T}\right) + \frac{3}{E_\pi} \coth\left(\frac{E_\pi}{2T}\right) - \frac{4N_c N_f}{E_q} [1 - N_q(T, \mu; \Phi, \bar{\Phi}) - N_{\bar{q}}(T, \mu; \Phi, \bar{\Phi})] \right\}, \quad (1)$$

where  $k$  is the infrared cut-off scale. The quasi-particle energies are given by,  $i = q, \pi, \sigma$ ,

$$E_i = \sqrt{k^2 + m_i^2}, \quad m_q^2 = h^2\phi^2, \quad m_\pi^2 = 2\Omega'_k, \quad m_\sigma^2 = 2\Omega'_k + 4\phi^2\Omega''_k, \quad (2)$$

with  $\phi = (\sigma, \vec{\pi})$  and primes denote derivatives with respect to  $\phi^2$ . The Polyakov-loop enhanced quark/anti-quark occupation numbers read

$$N_q(T, \mu; \Phi, \bar{\Phi}) = \frac{1 + 2\bar{\Phi}e^{(E_q-\mu)/T} + \Phi e^{2(E_q-\mu)/T}}{1 + 3\bar{\Phi}e^{(E_q-\mu)/T} + 3\Phi e^{2(E_q-\mu)/T} + e^{3(E_q-\mu)/T}} \quad (3)$$

and  $N_{\bar{q}}(T, \mu; \Phi, \bar{\Phi}) \equiv N_q(T, -\mu; \bar{\Phi}, \Phi)$ . Eq. (1) as it stands is still a flow equation for the free energy of full QCD with the approximation of a classical dispersion of quarks and mesons. The gluons have been integrated out, their dynamics is directly stored in the glue Polyakov-loop potential  $\Omega_{\text{glue}}$  as well as the initial conditions for  $\Omega_\Lambda$ . Hence, only the matter part  $\Omega_{\text{matter},k}$  depends on the cut-off scale  $k$ , to wit  $\partial_k\Omega_{\text{QCD},k} = \partial_k\Omega_{\text{matter},k}$ . This leads us to the final expression for the QCD free energy  $\Omega_{\text{QCD}} = \Omega_{\text{QCD},k=0}$ ,

$$\Omega_{\text{QCD}}(\sigma, \vec{\pi}, \Phi, \bar{\Phi}) = \Omega_{\text{glue}}(\Phi, \bar{\Phi}) + \int_\Lambda^0 dk \partial_k \Omega_{\text{matter},k}(\sigma, \vec{\pi}, \Phi, \bar{\Phi}) + \Omega_{\text{matter},\Lambda}(\sigma, \vec{\pi}, \Phi, \bar{\Phi}). \quad (4)$$

The flow equation (1) is indeed that of the matter sector of the two-flavour QCD flow derived in [12] with  $\Phi = \Phi(A_0)$ . At sufficiently large initial cut-off scale  $\Lambda$  the initial matter part of the free energy,  $\Omega_{\text{matter},\Lambda}$ , is just a local Yukawa-type action of quarks and mesons, its parameters are fixed with phenomenology in the vacuum with  $f_\pi$ ,  $m_\pi$  and  $m_\sigma$ . We also remark that the independence of the full free energy from the initial cut-off scale  $\Lambda$ , that is  $\partial_\Lambda\Omega_{\text{QCD}} \equiv 0$ , enforces  $\Lambda$  dependent terms in  $\Omega_{\text{matter},\Lambda}$ . These terms can be determined from the flow at  $\Lambda$ , see the reviews [20, 21, 22, 23, 24, 25]. Phenomenologically, they can be understood as the high-energy part of the vacuum fluctuations, see [34, 35].

In the following we present results based on the full integration of the flow of  $\Omega_{\text{QCD}}$  without any further approximation: the flow (1) is solved on

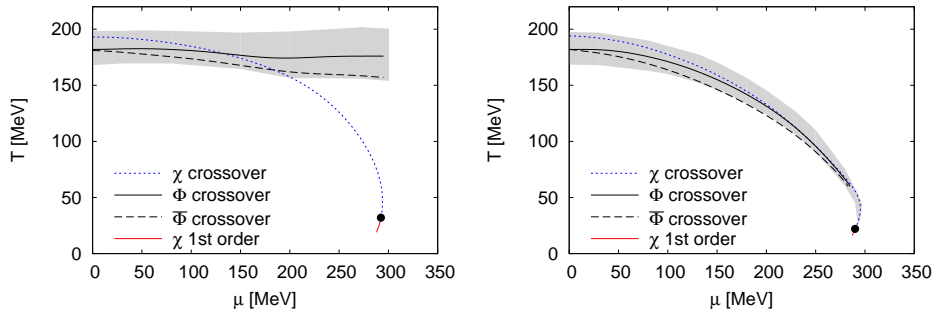


Fig. 3. Phase diagram with constant  $T_0$  (left) and with running  $T_0(\mu)$  (right).

a  $\sigma$ -grid for general fixed backgrounds  $\Phi$ ,  $\bar{\Phi}$ . Note in this context that the couplings in the initial condition  $\Omega_{\text{QCD},\Lambda}$  are insensitive to the choice of  $\Phi$ ,  $\bar{\Phi}$ . By mapping out the  $\Phi$ ,  $\bar{\Phi}$ -plane this provides us with the final result  $\Omega_{\text{QCD}}(\sigma, \vec{\pi}, \Phi, \bar{\Phi}) = \Omega_{\text{QCD},k=0}(\sigma, \vec{\pi}, \Phi, \bar{\Phi})$ . This goes beyond the approximation used in [13] where the flow was solved on the mean-field solutions  $\Phi(\sigma)$ ,  $\bar{\Phi}(\sigma)$ . It has been argued there that the latter already provides a quantitatively reliable approximation to the full solution and the present results fully confirm this argument. More details will be presented elsewhere [36]. The present computation allows us to solve the equations of motion for  $\Phi$ ,  $\bar{\Phi}$  and  $\sigma$  without further approximations and hence to determine the free energy and other thermodynamic quantities.

The above discussion of the Polyakov loop potential only exemplifies how results obtained within the first principle FRG approach to QCD can be used in order to constrain model computations. It is by no means restricted to the current example and provides a way of systematically improving the models towards full QCD. Moreover, lattice results provide further input and in particular also help to improve the quantitative precision of the QCD flows. In our opinion, in combination this opens a systematic path of mapping out the phase diagram of QCD.

### 3. Phase structure at physical pion masses

Fig. 3 summarizes our findings for the two-flavour phase structure at physical pion masses,  $m_\pi = 138$  MeV, and for a constant  $T_0$  (left) and running  $T_0(\mu)$  parameter (right). The gray band denotes the width of the temperature derivative of the Polyakov-loop (solid black line) at 80% of its maximum height. The dashed black line labels the inflection point of the conjugate Polyakov-loop. Both Polyakov-loop transitions, in the following referred to as deconfinement transition, are crossovers at low  $\mu$ . With a constant  $T_0$  (left panel), we find an almost  $\mu$  independent deconfinement

temperature which is slightly below the chiral crossover (dotted blue line). At  $\mu \approx 200$  MeV the chiral and deconfinement transitions start to deviate and we find a region in the phase diagram where chiral symmetry is partially restored and confinement still persists. The picture changes when we include the matter back-reaction to the gluonic sector via a running  $T_0(\mu)$  (right panel). In this case, both transitions lie close to each other throughout the whole phase diagram and no room for a chirally restored and confined phase is left. Remarkably, a similar scenario was found in another recent two-flavour non-perturbative functional study with Dyson-Schwinger equations [37].

With or without matter back-coupling to the YM system, we always find a critical endpoint around  $(T^{\text{CEP}}, \mu^{\text{CEP}}) \approx (20 \dots 30, 290)$  MeV. The endpoint is located at low temperatures, which results from the inclusion of quark and meson fluctuations. In standard mean-field calculations, where the mesonic fluctuations are ignored,  $T^{\text{CEP}}$  is typically much higher [38]. Already the inclusion of the fermion vacuum fluctuations lead to much lower  $T^{\text{CEP}}$  values, see e.g. [39, 35, 34].

Note however, that the present approximation lacks accuracy at large chemical potential. There we expect baryonic degrees of freedom to be important. We indeed envisage that it is not so much the baryonic off-shell fluctuations but rather their importance for the true ground state that matters. Diquark fluctuations, however, may play a quantitative rôle. These considerations are supported by the findings in two-colour QCD, see e.g. [40, 41, 42, 43]. Hence we conclude that the present approximation lacks predictive power for  $\mu/T \sim 2$ . In turn, for smaller ratios it is reliable and as our computations show, there is no sign of a critical point in this regime. More details on this matter will be presented in [36].

#### 4. Chiral limit

In the chiral limit, chiral symmetry is exactly restored at high temperatures and/or densities and the chiral transition is a phase transition and not a crossover, see Fig. 4 (left panel). At  $\mu = 0$  we encounter a second-order phase transition, in agreement with  $O(4)$ -universality arguments [44]. At large chemical potential, we find an interesting phase separation: the second-order chiral transition splits into two branches for decreasing temperatures. The inner branch (at smaller chemical potential) shows the inward-bending behaviour characteristic for studies including thermal and quantum fluctuations. It turns into a first-order transition for smaller temperatures with a critical endpoint. The outer branch bends outwards and stays of second-order. This behaviour is in agreement with previous FRG findings in the pure quark-meson model in the chiral limit, cf. [39]. Interestingly, the

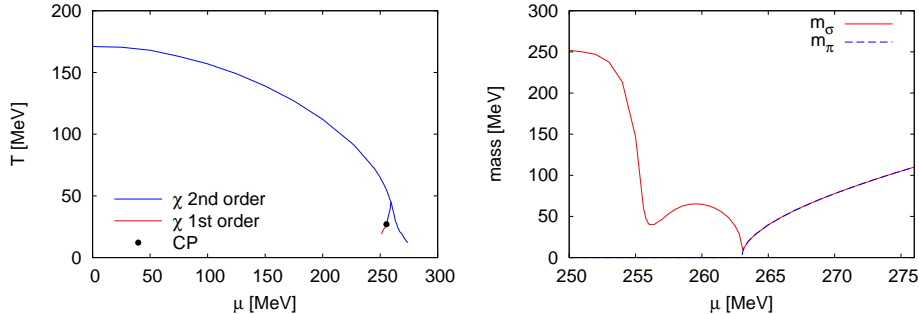


Fig. 4. Left: Phase diagram for the chiral transition in the chiral limit. Right: Meson masses in the chiral limit at  $T = 30$  MeV.

critical temperature of the endpoint  $T^{\text{CEP}}(\mu^{\text{CEP}})$  is almost independent of the explicit symmetry breaking, i.e., independent of the pion mass. This is in contrast to  $T^{\text{CEP}}(\mu = 0)$  which for decreasing pion mass also decreases. Hence, the endpoint lies in the same temperature range as for physical pion masses. In turn, the critical chemical potential  $\mu^{\text{CEP}}$  changes with decreasing pion mass to smaller values. This can be understood as follows: the chemical potential at which the phase transition line hits the  $\mu$ -axis is related to the value of the quark mass and also to the sigma meson mass. Both masses are smaller in the chiral limit, cf. also [45].

The transition splitting is accompanied by two minima in the sigma meson mass as a function of the chemical potential. This is shown in Fig. 4 (right panel) for a temperature above the endpoint. In contrast to the sigma meson mass, the pions stay massless until chiral symmetry is completely restored, which happens at the outer transition branch. For larger chemical potential, both meson masses degenerate due to the restored chiral symmetry.

## 5. Small pion masses

As previously shown, the chiral limit phase structure has peculiar features at large chemical potential that are not present at physical pion mass. In the following, we demonstrate how the chiral limit is connected to the physical mass point and study the influence of an increasing pion mass on the chiral transition splitting in the phase diagram.

For a non-vanishing explicit chiral symmetry breaking parameter, the second-order chiral transition at moderate chemical potential turns into a crossover. Apart from this, the phase structure remains qualitatively the same. At small pion masses, for example  $m_\pi = 50$  MeV, the splitting in the chiral transition persists and we find a critical endpoint on the inner branch,



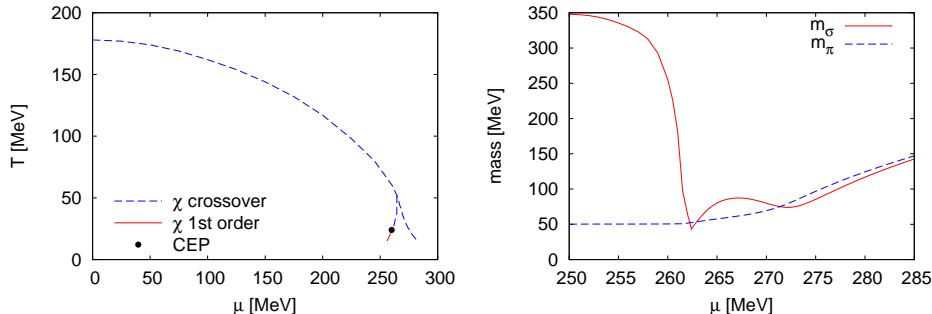


Fig. 5. Similar to Fig. 4, but for  $m_\pi = 50$  MeV.

again around  $T_c \approx 20 - 30$  MeV, cf. Fig. 5 (left). For smaller temperatures the transition is of first-order. The outer branch remains a crossover for all temperatures. The sigma meson mass as a function of chemical potential shows a behaviour similar to the chiral limit. The second minimum is still visible, but much weaker, see Fig. 5 (right). For a larger explicit symmetry breaking this effect is washed out. Furthermore, the inflection point of the chiral condensate, which determines the transition line, is also smeared out at larger pion masses. At physical pion masses no splitting is observed anymore, cf. Fig. 3.

## 6. Pressure

In order to understand the properties of the chiral splitting region in the phase diagram in more detail, we also compute the pressure in this regime. In Fig. 6 we show the pressure normalized by its Stefan-Boltzmann value as a function of  $\mu$  for  $m_\pi = 50$  MeV at the fixed temperature  $T = 30$  MeV. Clearly, the pressure in the splitting regime is not a monotonically rising function. A local minimum in the scaled pressure appears at about the chemical potential where the sigma meson mass has its local maximum. Only for chemical potential beyond the second transition branch the pressure increases significantly. Note however, that the dropping of the pressure for these densities is unphysical and hints at some shortcoming of the Polyakov-loop implementation in PQM/PNJL models. As already pointed out above, the coefficients of the effective Polyakov-loop potential are fitted to lattice data at vanishing chemical potential. Some density aspects of the matter back-coupling are included by our modifications where  $T_0$  has been replaced by  $T_0(N_f, \mu)$ , but a fully dynamical treatment within the FRG is still missing.

Indeed, the slope of the used effective Polyakov-loop potential ansatz is known to be steeper than the corresponding potential in full QCD, see

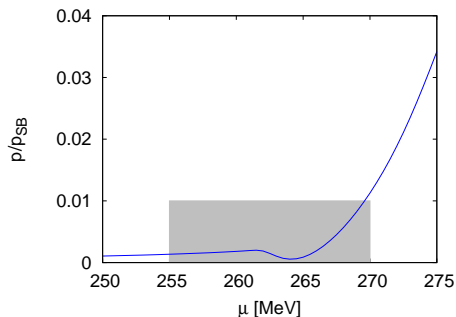


Fig. 6. Pressure in the splitting region,  $T = 30$  MeV, for  $m_\pi = 50$  MeV.

[12, 33, 2] which might result in such an unphysical behaviour. In any case we observe that a small change in the parameters of the Polyakov loop potential lead to qualitative changes in the regime under discussion. Hence, in order to get a more realistic description of the QCD phase diagram, in particular in this density regime, the full dynamics of the glue potential  $\Omega_{\text{glue}}$  has to be taken into account. In our opinion this, together with the inclusion of baryonic and diquark degrees of freedom already discussed above, will give us access to the highly interesting nuclear matter regime at low temperature and relatively large densities.

## 7. Conclusion and Outlook

In the present contribution we have discussed the effects of quantum and thermal fluctuations as well as the pion mass sensitivity of the phase structure of QCD. This is done within the dynamical Polyakov-extended quark-meson model where fluctuations are included via the functional renormalization group. We have also argued that the PQM model can be understood as a well-controlled approximation to first principle QCD. The precise knowledge of the approximations involved can be used to systematically improve the PQM model towards full QCD by successively fixing the model parameters with QCD input. Specifically, we have considered the back-coupling of quarks to the glue sector of QCD which results in a  $N_f$ - and  $\mu$  dependent modification of the  $T_0$  parameter in the Polyakov-loop potential.

At physical pion masses, the FRG phase diagram exhibits a critical endpoint whose location is pushed towards large chemical potential and low temperature in comparison with a standard mean-field approximation. This emphasizes the significant influence of fluctuations. We could rule out the emergence of an endpoint for small chemical potential below  $\mu/T \approx 2$ .

In the chiral limit, a splitting of the chiral transition line at large chemical potential and below  $T < 50$  MeV could be confirmed within our trun-

cation. Two transition branches with different transition orders emerge for small temperatures. On the inner branch, a second-order critical endpoint as the endpoint of the first-order transition line could be determined. Within the splitting region chiral symmetry is still broken.

Interestingly, the area of the splitting region is not very sensitive to the pion mass. For a small pion mass the splitting phenomenon still persists and the critical temperature of the endpoint is almost pion mass independent. For non-vanishing pion masses the chiral transition changes from the chiral  $O(4)$  universality to a crossover. Since fluctuations weaken the chiral phase transition the crossover is in addition washed out and disappears when we approach physical pion masses. However, some remnants of the second transition branch are still present in the chiral condensate at physical pion masses.

The investigation of the thermodynamics in the splitting region might shed more light on the nature of the different transitions and the emergence of a critical endpoint. Concerning the pressure in this region we found that the Polyakov-loop potential has some deficiencies at low temperature and large chemical potential. Within the splitting region, the slope of the normalized pressure as a function of chemical potential becomes negative, which is an unphysical behaviour and hampers the computation of other thermodynamic quantities there. However, in this regime of the phase diagram baryonic degrees of freedom are of importance but have been neglected so far.

Furthermore, the inclusion of the matter back-coupling to the glue sector favours the coincidence of chiral and Polyakov-loop transition lines also at larger chemical potential. This is in clear contradistinction to the mean-field results where one observes a separation of the two transitions. This, together with large- $N_c$  investigations, has been used as an indication for a quarkyonic phase, where chiral symmetry is restored but matter still confined. Given the intricacies related with the interpretation of the Polyakov loop as an order parameter for the confinement/deconfinement phase transition at finite density, we merely note that our results with fluctuations cast some doubt on the support provided by the mean-field investigations with Polyakov-extended models. Seemingly, it is the lack of matter back-coupling in these investigations which triggers the separation of the transition lines. Note also that this missing back-coupling is built-in in the large- $N_c$  limit.

In summary, the dynamical Polyakov-loop extended quark-meson model provides a good approximation to full QCD at small densities. For densities beyond  $\mu/T > 2$  the present approximation has to be extended to include baryonic degrees of freedom, the effects of in-medium propagation and that of multi-scatterings in a dense medium.

### Acknowledgements

TKH is recipient of a DOC-fFORTE-fellowship of the Austrian Academy of Sciences and supported by the FWF doctoral program DK-W1203-N16. JMP acknowledges support by Helmholtz Alliance HA216/EMMI and BJS by the Helmholtz Young Investigator Group No. VH-NG- 332.

### REFERENCES

- [1] B. Friman *et al.*, Lect.Notes Phys. **814**, 1 (2011).
- [2] J. M. Pawlowski, AIP Conf.Proc. **1343**, 75 (2011), 1012.5075.
- [3] O. Philipsen, (2011), 1111.5370.
- [4] S. Borsanyi *et al.*, JHEP **1011**, 077 (2010), 1007.2580.
- [5] HotQCD collaboration, A. Bazavov and P. Petreczky, J.Phys.Conf.Ser. **230**, 012014 (2010), 1005.1131.
- [6] K. Fukushima and T. Hatsuda, Rept.Prog.Phys. **74**, 014001 (2011), 1005.4814.
- [7] B.-J. Schaefer, J. M. Pawlowski, and J. Wambach, Phys.Rev. **D76**, 074023 (2007), 0704.3234.
- [8] E. Megias, E. Ruiz Arriola, and L. Salcedo, Phys.Rev. **D74**, 065005 (2006), hep-ph/0412308.
- [9] C. Ratti, M. A. Thaler, and W. Weise, Phys.Rev. **D73**, 014019 (2006), hep-ph/0506234.
- [10] K. Fukushima, Phys.Lett. **B591**, 277 (2004), hep-ph/0310121.
- [11] A. Dumitru, Y. Hatta, J. Lenaghan, K. Orginos, and R. D. Pisarski, Phys.Rev. **D70**, 034511 (2004), hep-th/0311223.
- [12] J. Braun, L. M. Haas, F. Marhauser, and J. M. Pawlowski, Phys.Rev.Lett. **106**, 022002 (2011), 0908.0008.
- [13] T. K. Herbst, J. M. Pawlowski, and B.-J. Schaefer, Phys.Lett. **B696**, 58 (2011), 1008.0081.
- [14] P. N. Meisinger and M. C. Ogilvie, Phys.Lett. **B379**, 163 (1996), hep-lat/9512011.
- [15] J. Braun and A. Janot, Phys.Rev. **D84**, 114022 (2011), 1102.4841.
- [16] V. Skokov, B. Stokic, B. Friman, and K. Redlich, Phys.Rev. **C82**, 015206 (2010), 1004.2665.
- [17] V. Skokov, B. Friman, and K. Redlich, Phys.Rev. **C83**, 054904 (2011), 1008.4570.
- [18] K. Morita, V. Skokov, B. Friman, and K. Redlich, Phys.Rev. **D84**, 076009 (2011), 1107.2273.
- [19] V. Skokov, (2011), 1112.5137.
- [20] D. F. Litim and J. M. Pawlowski, World Sci. , 168 (1999), hep-th/9901063.

- [21] J. Berges, N. Tetradis, and C. Wetterich, Phys.Rept. **363**, 223 (2002), hep-ph/0005122.
- [22] J. M. Pawłowski, Annals Phys. **322**, 2831 (2007), hep-th/0512261.
- [23] H. Gies, (2006), hep-ph/0611146.
- [24] B.-J. Schaefer and J. Wambach, Phys.Part.Nucl. **39**, 1025 (2008), hep-ph/0611191.
- [25] J. Braun, J.Phys.G **G39**, 033001 (2012), 1108.4449.
- [26] B.-J. Schaefer, M. Wagner, and J. Wambach, Phys.Rev. **D81**, 074013 (2010), 0910.5628.
- [27] B.-J. Schaefer, Phys.Atom.Nucl. **75** (2012), in press, 1102.2772.
- [28] J. Braun, H. Gies, and J. M. Pawłowski, Phys.Lett. **B684**, 262 (2010), 0708.2413.
- [29] H. Gies and C. Wetterich, Phys.Rev. **D65**, 065001 (2002), hep-th/0107221.
- [30] H. Gies and C. Wetterich, Phys.Rev. **D69**, 025001 (2004), hep-th/0209183.
- [31] S. Floerchinger and C. Wetterich, Phys.Lett. **B680**, 371 (2009), 0905.0915.
- [32] J. Braun, Eur. Phys. J. **C64**, 459 (2009), 0810.1727.
- [33] L. M. Haas, J. Braun, and J. M. Pawłowski, AIP Conf.Proc. **1343**, 459 (2011), 1012.4735.
- [34] V. Skokov, B. Friman, E. Nakano, K. Redlich, and B.-J. Schaefer, Phys.Rev. **D82**, 034029 (2010), 1005.3166.
- [35] B.-J. Schaefer and M. Wagner, Phys.Rev. **D** (2012), in press, 1111.6871.
- [36] T. K. Herbst, J. M. Pawłowski, and B.-J. Schaefer, in preparation (2012).
- [37] C. S. Fischer, J. Luecker, and J. A. Mueller, Phys.Lett. **B702**, 438 (2011), 1104.1564.
- [38] B.-J. Schaefer and J. Wambach, Phys.Rev. **D75**, 085015 (2007), hep-ph/0603256.
- [39] B.-J. Schaefer and J. Wambach, Nucl.Phys. **A757**, 479 (2005), nucl-th/0403039.
- [40] N. Strodthoff, B.-J. Schaefer, and L. von Smekal, (2011), 1112.5401.
- [41] T. Brauner, K. Fukushima, and Y. Hidaka, Phys.Rev. **D80**, 074035 (2009), 0907.4905.
- [42] C. Ratti and W. Weise, Phys.Rev. **D70**, 054013 (2004), hep-ph/0406159.
- [43] S. Hands, I. Montvay, L. Scorzato, and J. Skullerud, Eur.Phys.J. **C22**, 451 (2001), hep-lat/0109029.
- [44] R. D. Pisarski and F. Wilczek, Phys.Rev. **D29**, 338 (1984).
- [45] B.-J. Schaefer and M. Wagner, Phys.Rev. **D79**, 014018 (2009), 0808.1491.